# Numerical modelling of meso-scale finish machining with finite edge radius tools

Tugrul Özel* and Erol Zeren

Department of Industrial and Systems Engineering,
Rutgers University,
Piscataway, NJ 08854-8018, USA
E-mail: ozel@rci.rutgers.edu
*Corresponding author

**Abstract:** Finite edge radius plays a significant role in finish machining processes when the undeformed chip thickness is often less than a few hundred microns and comparable to the size of the cutting edge. At suboptimal cutting speeds, edge radius tools may induce deeper subsurface plastic deformation, increase microhardness through work-hardening and mostly due to the ploughing of the cutting edge. Once tool edge radius, tool geometry and cutting conditions are optimised, finish machining can produce superior surface properties than surfaces generated by grinding and polishing. In this paper, an Arbitrary Lagrangian Eulerian (ALE)-based numerical modelling is employed. The Johnson-Cook (J-C) plasticity model is used to describe the work material behaviour. A detailed friction modelling at the tool-chip interface is also carried. Numerical modelling revealed stress and temperature fields induced by the finite edge radius cutting edge on the machined subsurface.

**Keywords:** arbitrary Lagrangian Eulerian method; ALE; meso/micromachining; finite edge radius tools.

**Reference** to this paper should be made as follows: Özel, T. and Zeren, E. (2007) 'Numerical modelling of meso-scale finish machining with finite edge radius tools', *Int. J. Machining and Machinability of Materials*, Vol. 2, Nos. 3/4, pp.451–468.

**Biographical notes:** Tugrul Özel is a PhD in Mechanical Engineering from The Ohio State University in 1998. He is an Assistant Professor of Industrial and Systems Engineering at Rutgers University and the Director of Manufacturing Automation and Research Laboratory. His current research interest includes computational modelling of manufacturing processes, machining, process control and optimisation and micro/nano manufacturing. He has over 10 years of experience in teaching and researching about manufacturing. He has been a reviewer, Guest Editor and an Editorial Board Member for several international journals. He has published over 50 refereed papers in international journals and conferences.

Erol Zeren is an MSc in Industrial Engineering from Rutgers University and is at Seagate Technologies Inc., Minnesota, USA. His main research interests include high speed machining and CAD/CAM. He has published several research papers in international conferences.

## 1 Introduction

There is strong demand for the low feed rate machining where the undeformed chip thickness is comparable to the size of the cutting edge radius such as in finish high-speed machining (Byrne et al., 2003) and finish hard turning (Tönshoff et al., 2000) at meso scale (100 μm–1 mm) and micromachining (Dornfeld et al., 2006; Weule et al., 2001) at microscale (0.1–100 μm). Numerical modelling of machining processes is continuously attracting researchers for better understanding of chip formation mechanisms, heat generation in cutting zone, tool-chip interfacial frictional characteristics and quality and integrity of the machined surfaces. In predictive process engineering for machining processes, prediction of physics related process field variables such as temperature and stress fields becomes highly important. Finite edge radius tool geometry particularly influences surface quality and integrity on machined features as well as tool life and process viability. Continuum-based finite element analysis and numerical models are essential to investigate the influence of tool edge size, geometry, material and coating on the surface integrity especially machining induced stress and temperature fields. This paper aims to review the numerical modelling studies conducted in the past and to introduce an Arbitrary Lagrangian Eulerian (ALE) model for the meso-scale finish machining process to predict the stress and temperature fields on the machined subsurface.

### *1.1 Review of numerical modelling of machining*

In continuum-based finite element modelling, there are two types of analysis in which a continuous medium can be described: Eulerian and Lagrangian. In a Lagrangian analysis, the computational grid deforms with the material whereas in a Eulerian analysis this is fixed in space. The Lagrangian calculation embeds a computational mesh in the material domain and solves for the position of the mesh at discrete points in time. In those analyses, two distinctive methods, the implicit and explicit time integration techniques can be utilised. The implicit technique is more applicable for solving linear static problems while explicit method is more suitable for non-linear dynamic problems.

A majority of earlier numerical models have relied on the Lagrangian formulation (Komvopoulos and Erpenbeck, 1991; Lin and Lin, 1992; Shih, 1995; Strenkowski and Carroll, 1985; Usui and Shirakashi, 1982; Zhang and Bagchi, 1994), whereas some of the numerical models utilised the Eulerian formulation (Strenkowski and Carroll, 1986). However, it was evident that the Lagrangian formulation required a criterion for separation of the undeformed chip from the workpiece. For this purpose, several chip separation criteria such as strain energy density, effective strain criteria have been implemented as exclusively reported by Black and Huang (1996). Updated Lagrangian implicit formulation with continuous remeshing without using chip separation criteria has also been used in simulation of continuous and segmented chip formation in machining processes (Baker et al., 2002; Ceretti et al., 1996; Klocke et al., 2001; Leopold et al., 1999; Madhavan et al., 2000; Marusich and Ortiz, 1995; Özel and Altan, 2000; Sekhon and Chenot, 1992). ALE technique combines the features of pure Lagrangian and Eulerian analysis. ALE formulation is also utilised in simulating machining to avoid frequent remeshing for chip separation (Adibi-Sedeh and Madhavan, 2003; Haglund et al., 2005; Rakotomalala et al., 1993; Movahhedy et al., 2002;

Movahhedy et al 2000; Olovsson et al., 1999; Özel and Zeren, 2005a,b). Explicit dynamic ALE formulation is a very efficient technique for simulating highly non-linear problems involving large localised deformations and under changing contact conditions as those experienced in machining. The explicit dynamic procedure performs a large number of small time increments efficiently. The adaptive meshing technique does not alter elements and connectivity of the mesh. This technique allows flow boundary conditions whereby only a small part of the workpiece in the vicinity of the tool tip needs to be modelled. Authors work in numerical modelling with ALE technique has been extended to meso-scale finish machining in this paper.

Friction in meso-scale machining plays an important role in thermo-mechanical processing of the machined work surface. Many publications about friction in machining can be found in literature (Dirikolu et al., 2001; Haglund et al., 2005; Özel, 2006; Yang and Liu, 2002). The most common approach in modelling friction is to use an average coefficient of friction. Late models consist of a sticking region at tool rake face for which the friction force is constant, and a sliding region for which friction force varies linearly according to Coulomb's law.

Numerical modelling of finish machining is essential to predict accurate tool forces, stress, temperature, strain and strain rate fields. Recent numerical modelling studies in machining reported in the literature include simulation of machining non-homogenous materials (Chuzhoy et al., 2003), simulation of machining hardened steels (Guo and Liu, 2002; Liu and Guo, 2000; Yang and Liu, 2002), investigations on the effects of tool edge geometries (Guo and Wen, 2005; Movahhedy et al., 2002; Özel, 2003; Yen et al., 2004) and the effects of work material models on the chip formation and temperature predictions (Davies et al., 2003; Deshayes et al., 2004). Edge geometry of the tool affects the depth of plastic deformation zone underneath the tool and has a dominant influence on machining induced stresses on the finished surface. Earlier numerical modelling studies have relied on chip-workpiece separation criteria around the cutting edge which undermined the effects of cutting edge geometry on the field variables (strain, stress, temperatures, etc.) of the machined surface. In this study, work material is allowed to flow around the round edge of the cutting tool and therefore the physical process is simulated more realistically and the field variables are obtained accordingly.

## *1.2 Characteristics of meso-scale machining*

Most cutting tools used for finish machining have a finite-edge radius and cannot be considered sharp. According to Zorev (1966), the radius of the cutting edge does not affect the cutting process if the ratio of uncut chip thickness to the edge radius ($t_u/r_e$) is equal or greater to ten. In meso-scale cutting, where the uncut chip thickness is very small this ratio becomes close to one. Outeiro and Astakhov (2005) have used this ratio introduced to describe relative tool sharpness. The specific cutting forces depend mostly on this ratio especially when they are comparable in size. This so called size effect is originally observed in ultra precision diamond cutting. According to Lucca and Seo (1993), owing to the highly localised shearing, the specific cutting forces in ultra precision cutting are almost twice that of in conventional cutting. A minimum uncut chip thickness is observed in microcutting where tool engagement with workpiece only result in chip formation when uncut chip thickness is greater $t_u > = t_{c\_\min}$ (Ikawa et al., 1992). Both size effect and minimum chip thickness are also experimentally investigated in

micro machining (Melkote and Endres, 1998; Schmidt and Tritschler, 2004). Further discussion on size effect and minimum chip thickness can be found in Joshi and Melkote (2004) and Liu et al. (2006).

The cutting behaviour and the mechanism of chip formation are also known to depend on crystallographic factors, such as orientation, slip systems and the mobile dislocation density of the workpiece (Lee and Zhou, 1993). Because the uncut chip thickness (usually less than 100 μm) in meso-scale machining is comparable to the average grain size of a polycrystalline aggregate (e.g. between 1.5 and 150 μm for ferritic steels), cutting is performed within the grains as illustrated in Figure 1. The polycrystalline material, which can be considered to be an isotropic and homogeneous continuum in conventional analysis, must be treated as a series of single crystals with random orientations. Single crystals are known to be highly anisotropic in their physical and mechanical properties. Therefore, the crystallographic orientation of the substrate material will exert a significant influence on the microscale machining process (Lee and Zhou, 1993). Our current understanding of the mechanics of the cutting problem in such a micro region of the crystal is still far from perfect. Some problems still remain unsolved because the meso/microscale cutting mechanism is complex. Therefore, meso-scale machining conditions can be defined as where a relation of 1 μm ≤ $d < r_e < t_u \leq 100$ μm holds.

**Figure 1** Size comparison in meso-scale orthogonal cutting

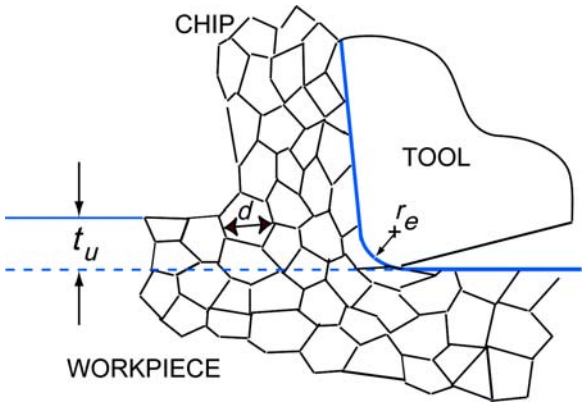


## 2 Numerical modelling of meso-scale finish machining

### *2.1 Work material model*

Accurate and reliable flow stress models are considered highly necessary to represent work material constitutive behaviour under machining conditions. A number of empirical and semi-empirical constitutive models have been developed to model flow stress with certain accuracy in machining (Özel and Zeren, 2006). Most of these constitutive models are based on a range of assumptions to avoid the prevailing complexities of stress state exist in machining. The microstructure and phase transformation also play a significant role on flow stress behaviour during finish machining where small-undeformed chip loads are taken. The strain rate and temperature coupling effect is especially important at

high cutting speeds where thermal softening becomes more dominant due to increased heat generation. A detailed discussion about work material considerations is given in Astakhov (1999).

Among many other material constitutive models, model by Johnson and Cook (1983) is widely used for high-strain rate applications. This constitutive model describes the flow stress of a material with the product of strain, strain rate and temperature effects that are individually determined as given in Equation 1. In the Johnson-Cook (J-C) model, the constant $A$ is yield strength of the material at room temperature and a strain rate of 1/s and $\bar{\varepsilon}$ represents the plastic equivalent strain. The strain rate $\dot{\bar{\varepsilon}}$ is normalised with a reference strain rate $\dot{\bar{\varepsilon}}_0$. Temperature term in the J-C model reduces the flow stress to zero at the melting temperature of the work material, leaving the constitutive model with no temperature effect. Although this material model is determined using a simple state of stress condition attained through Split Hopkinson Pressure Bar tests, for lack of a better material model, has been used in this study for meso-scale finish machining of three metal alloys. The constants of the J-C material for AISI 1045, AISI 4340 steels and Ti6Al4V titanium alloy are given in Table 1.

$$\bar{\sigma} = \left[ A + B\left(\bar{\varepsilon}\right)^n \right] \left[ 1 + C \ln\left( \frac{\dot{\bar{\varepsilon}}}{\dot{\bar{\varepsilon}}_0} \right) \right] \left[ 1 - \left( \frac{T - T_{\text{room}}}{T_{\text{melt}} - T_{\text{room}}} \right)^m \right] \tag{1}$$

**Table 1** The J-C material model constants

| *Material* | *A (MPa)* | *B (MPa)* | *n* | *C* | *m* | $T_{melt}$ *(°C)* |
|---|---|---|---|---|---|---|
| AISI 1045 (Jaspers and Dautzenberg, 2002) | 553.1 | 600.8 | 0.234 | 0.013 | 1.00 | 1460 |
| AISI 4340 (Ng et al., 2002) | 792.0 | 510.0 | 0.26 | 0.014 | 1.03 | 1520 |
| Ti6AlV4 (Meyer and Kleponis, 2001) | 862.5 | 331.2 | 0.34 | 0.012 | 0.8 | 1650 |

## *2.2 Friction at the tool-chip interface*

There are many studies in literature about stress distributions at the tool-chip interface as summarised in Astakhov (1999). Some of the experimental studies reported large scatter in these stresses while others suggested certain distributions. As originally proposed by Zorev (1966) and utilised by others (Childs et al., 2000; Dirikolu et al., 2001; Li, 1997; Özel and Altan, 2000; Usui and Shirakashi, 1982) normal and shear stress distributions can be assumed on the tool rake face as shown in Figure 2. According to this model, a sticking region forms in the tool-chip contact area near the cutting edge and the frictional shearing stress at the sticking region, $\tau_f$ can be assumed equal to an average shear flow stress at tool-chip interface in the chip, $k_{\text{chip}}$, $\tau_f = k_{\text{chip}}$. Over the remainder of the tool-chip contact area a sliding region forms and the frictional shearing stress can be determined by using a coefficient of friction, $\mu$. When the normal stress distribution over the rake face is fully defined and the coefficient of friction, $\mu$ is known, the frictional stress can be determined. Therefore, shear stress distribution on the tool rake face can be represented in two distinct regions:

**Figure 2** Normal and frictional stress distributions on the tool rake face

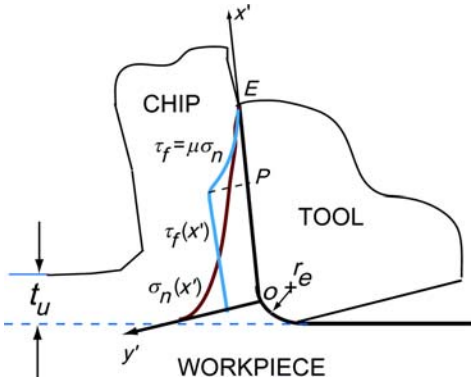


*Source*: Zorev (1966).

In the sticking region:

$$\tau_f(x') = k_{\text{chip}} \text{ and when } \mu\sigma_n(x') \geq k_{\text{chip}} \quad O < x' \leq P \tag{2a}$$

In the sliding region:

$$\tau_f(x') = \mu\sigma_n(x') \text{ and when } \mu\sigma_n(x') < k_{\text{chip}} \quad P < x' \leq E \tag{2b}$$

The calculated friction characteristics with the methodology explained in Özel and Zeren (2006) include parameters of the normal and frictional stress distributions on the rake face. Since the length of sticking region, $l_p$ and chip-tool contact length, $l_c$ are not implemented in the friction model in the continuum-based FEM simulations they are not given in Table 2. Instead, a limiting shear friction model is implemented with the limiting shear stress and friction coefficients are given in Table 2.

**Table 2** Friction characteristics when using an uncoated carbide-cutting tool

| | *AISI 1045 steel* | *AISI 4340* | *Ti6Al4V* |
|---|---|---|---|
| $k_{\text{chip}}$ (MPa) | 200 | 250 | 400 |
| $\mu$ | 0.5 | 0.5 | 0.5 |

## *2.3 ALE numerical modelling and adaptive meshing*

The essential and desired attributes of the continuum-based numerical models for meso-scale machining are:

1 the work material model should satisfactorily represent elastic plastic and thermo-mechanical behaviour of the work material deformations observed during machining process

2 numerical model should not require chip separation criteria that highly deteriorate the physical process simulation around the tool cutting edge especially when there is dominant tool edge geometry such as a round edge or a chamfered edge is present

3 interfacial friction characteristics on the tool-chip and tool-work contacts should be modelled highly accurately to account for additional heat generation and stress developments due to friction.

In this paper, a commercial software code, ABAQUS/Explicit v6.4 and explicit dynamic ALE modelling approach is used to conduct the numerical modelling of orthogonal cutting considering round tool edge geometry and all of the above attributes are successfully implemented in the model. The chip formation is simulated via adaptive meshing and plastic flow of work material. Therefore, there is no need for a chip separation criterion in the proposed numerical model.

The numerical model as shown in Figure 3 requires a predefined chip geometry. The chip surfaces are defined with the Lagrangian boundary conditions and the chip upper surface is defined with the Eulerian boundary conditions. Therefore, the chip flow is bound at a vertical position. However, the chip thickness and the chip-tool contact length gradually settle to their final size with the change in the deformation conditions as the cutting reaches its steady-state. The major drawback of this approach is that the predefined chip shape must be determined beforehand and entered into the numerical model. Similar ALE models were presented by Adibi-Sedeh and Mahdavan (2003), Haglund et al. (2005) and by the authors (Özel and Zeren, 2005a,b).

**Figure 3** Numerical model for ALE formulation (a) Eulerian and Lagrangian boundary conditions; (b) mesh with pre-defined chip, workpiece and tool dimensions

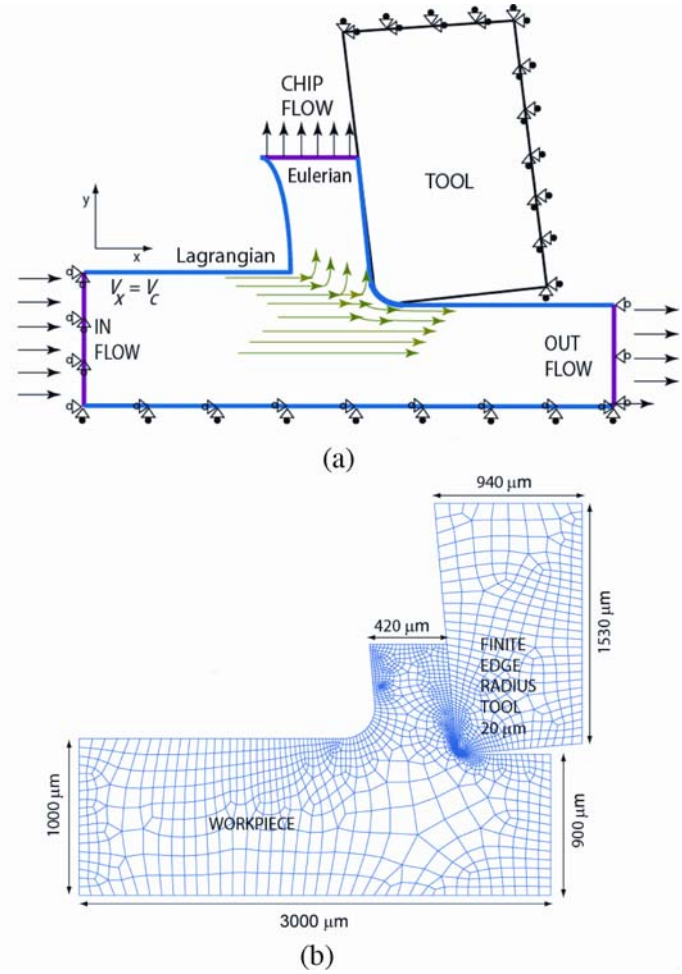

The workpiece is also modelled with the Eulerian boundaries from the both ends and with the Lagrangian boundaries at the top and the bottom. The top surface of the workpiece with the free boundaries reaches to the final deformed shape at the steady-state cutting.

In this ALE approach, the explicit dynamic procedure performs a large number of small time increments efficiently. The general governing equations are solved for both Lagrangian boundaries and Eulerian boundaries in the same fashion. The adaptive meshing technique does not alter elements and connectivity of the mesh. This technique combines the features of pure Lagrangian analysis in which the mesh follows the material, and Eulerian analysis in which the mesh is fixed spatially and the material flows through the mesh as explained earlier.

The thermo-mechanical numerical model is created by including workpiece thermal and mechanical properties, boundary conditions, contact conditions between tool and the workpiece as shown in Figure 3 and given in Tables 3 and 4. The workpiece and the tool model use four-node bilinear displacement and temperature (CPE4RT) quadrilateral elements and a plane strain assumption for the deformations in the orthogonal cutting process.

**Table 3** Work material properties

| *Work properties* | *AISI 1045* | *AISI 4340* | *Ti6Al4V* |
|---|---|---|---|
| Expansion (μm /m°C) | 11 | 1.23 | 4.7 |
| Density (g/cm$^3$) | 7.8 | 7.85 | 4.43 |
| Poisson's ratio | 0.3 | 0.22 | 0.34 |
| Specific heat (J/kg/°C) | 432.6 | 477 | 203 |
| Conductivity (W/m°C) | 47.7 | 44.5 | 6.7 |
| Young's modulus (GPa) | 200 | 208 | 113.8 |

**Table 4** Cutting conditions and tool material properties

| *Orthogonal cutting parameters* | |
|---|---|
| Cutting speed, $V_c$ (m/min) | 300 |
| Uncut chip thickness, $t_u$ (mm) | 0.1 |
| Width of cut, $w$ (mm) | 1 |
| Tool rake angle, $\alpha$ (degree) | –5 |
| Tool clearance angle (degree) | 5 |
| Tool edge radius, $\rho$ (mm) | 0.02 |
| *Carbide tool properties* | |
| Expansion (μm/m°C) | 4.7 |
| Density (g/cm$^3$) | 15 |
| Poisson's ratio | 0.2 |
| Specific heat (J/kg/°C) | 203 |
| Conductivity (W/m°C) | 46 |
| Young's Modulus (GPa) | 800 |

As it is shown in Figure 3 the workpiece was fixed at the bottom and at one end. The tool had a 20-micrometer edge radius and was modelled as elastic body with thermal conductivity.

The cutting process as a dynamic event causes large deformations in a few numbers of increments resulting in massive mesh distortion and termination of the simulation. It is highly critical to use adaptive meshing with fine tuned parameters to simulate the plastic flow over the round edge of the tool. Therefore the intensity, frequency and sweeping of the adaptive meshing are adjusted to most optimum setting for maintaining a successful mesh during the simulation of the meso-scale orthogonal cutting process.

The general equations of motion in explicit dynamic analysis are integrated by using explicit central difference integration rule with diagonal element mass matrices. The system equations become uncoupled so that each equation can be solved for explicitly. This makes explicit dynamic method highly efficient for non-linear dynamic problem such as metal cutting. During metal cutting, flow stress is highly dependent on temperature fields as we discussed earlier. Therefore, fully coupled thermal-stress analysis is required for accurate predictions in the simulations.

In summary, the explicit dynamic method is used mainly because it has the advantages of computational efficiency for large deformation and highly non-linear problems as experienced in machining. Meso/micromachining, as a coupled thermal-mechanical process, could generate heat to cause thermal effects that influence mechanical effects strongly. In the meantime, work material properties change significantly as strain rate and temperature changes. Thus, the fully coupled thermal-stress analysis, in which the temperature solution and stress solution are also carried out concurrently, is applied.

## 3 Results and discussions

The simulations based on the ALE-based numerical model for finish machining of AISI 1045, AISI 4340 and Ti6Al4V at the same cutting conditions were conducted and the chip formation process at the steady state was fully observed as shown in Figure 4.

**Figure 4** Chip formation and temperature distribution for machining of AISI 1045 steel

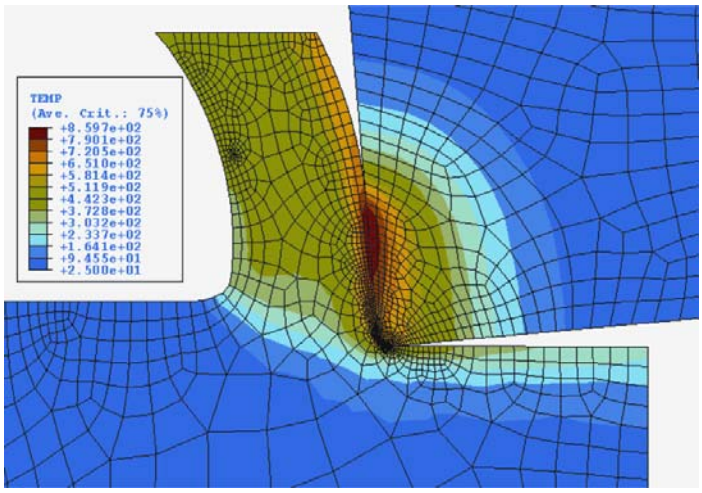

The heat generated at the secondary deformation zone and at tool-chip interface is conducted to the cutting tool. The radiation to the ambient is also allowed. Temperature distributions for machining of AISI 1045 and AISI 4340 steels and Ti6Al4V titanium alloy are obtained as shown in the Figures 4–6, respectively.

**Figure 5** Temperature distributions using ALE approach for machining of AISI 4340 steel

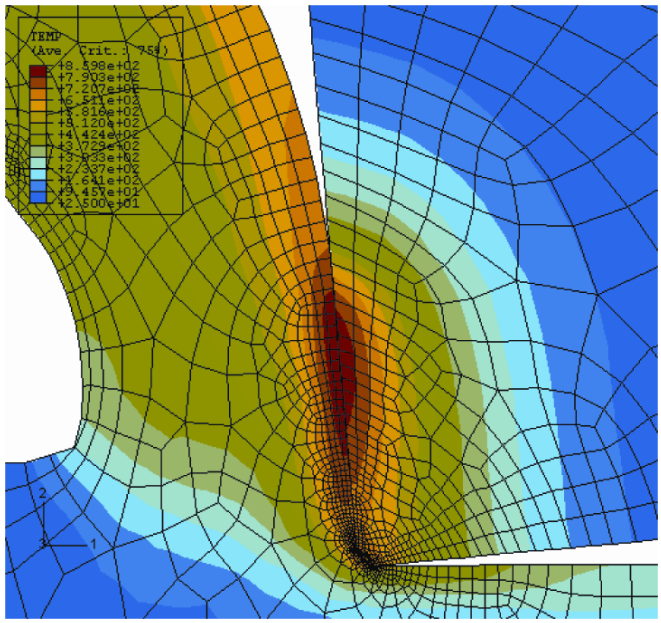


**Figure 6** Temperature distributions using ALE approach for machining of Ti6Al4V

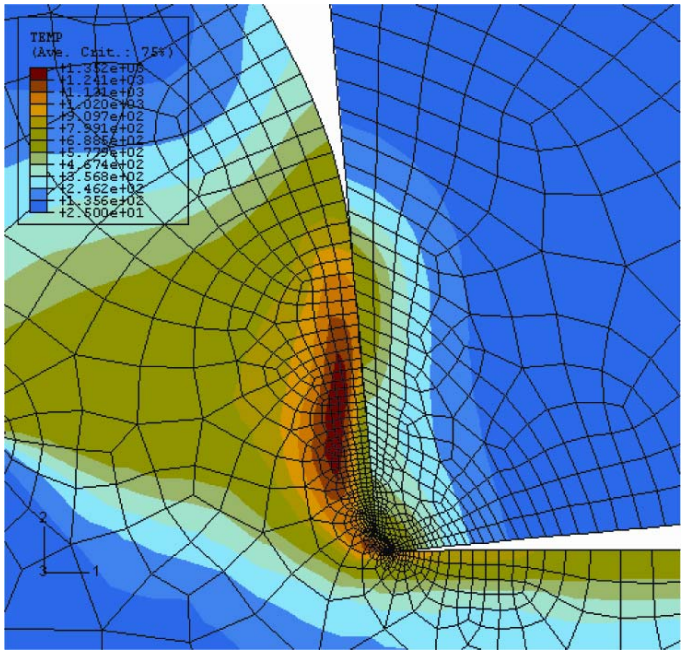

Temperature rises in the primary and secondary deformation zones are high and reach to a steady state very rapidly. It is highly noticeable that the maximum temperatures occur inside the chip due to the low thermal conductivity of the Ti6Al4V alloy, whereas the maximum temperatures are observed on the tool rake face in machining of steels.

The distributions of the predicted von Mises stress distributions are given in the Figures 7–9, respectively. The von Mises stress $\sigma_{xx}$ and $\sigma_{yy}$ also represent the stress distributions on the machined surface. From the simulation results it was observed that there exists a region of very high deformation rate around the round edge of the cutting tool.

**Figure 7** The Von Mises stress distributions in machining of AISI 1045 steel ($\times 10^6$ Pa, $t_u = 0.1$ mm, $V = 300$ m/min)

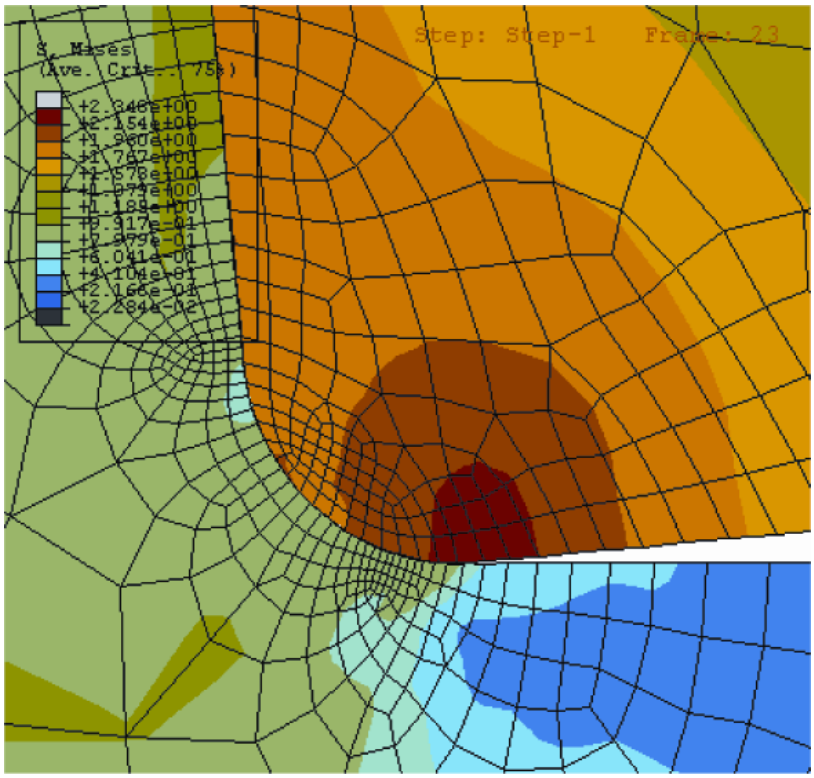


All three-work materials were utilised in the ALE-based FE simulations to observe the effects of machinability and also the field variables such as temperatures and stresses on the machined surfaces comparatively.

Machining induced residual stress profiles with respect to the depth beneath the machined surface for von Mises stresses, stress components $\sigma_{xx}$ and $\sigma_{yy}$ are also computed from the simulated stress fields.

A path prescribed underneath the round edge of the tool is tracked for obtaining the stress components and the temperature with respect to the depth inside the machined surface as shown in Figure 10.

**Figure 8** The Von Mises stress distributions in machining of AISI 4340 steel ($\times 10^6$ Pa, $t_u = 0.1$ mm, $V = 300$ m/min)

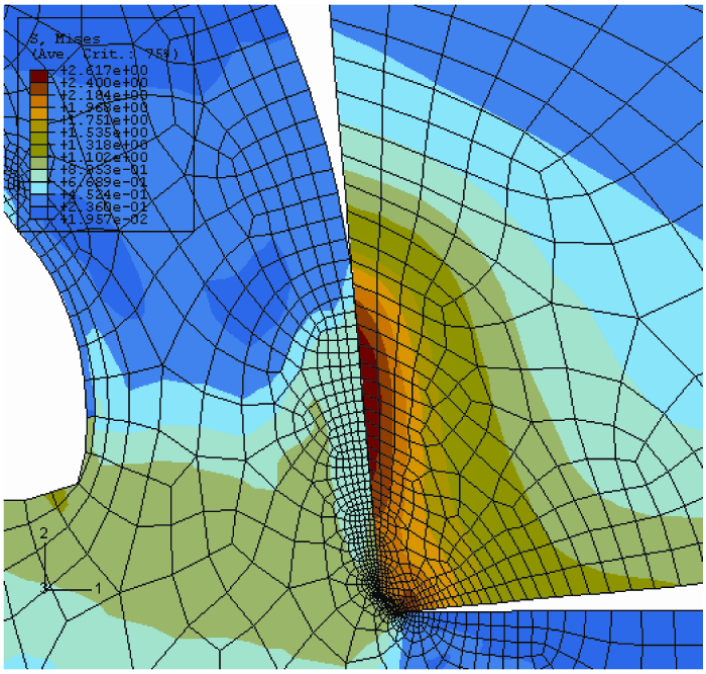


**Figure 9** The Von Mises stress distributions in machining of Ti6Al4V ($\times 10^6$ Pa, $t_u = 0.1$ mm, $V = 300$ m/min)

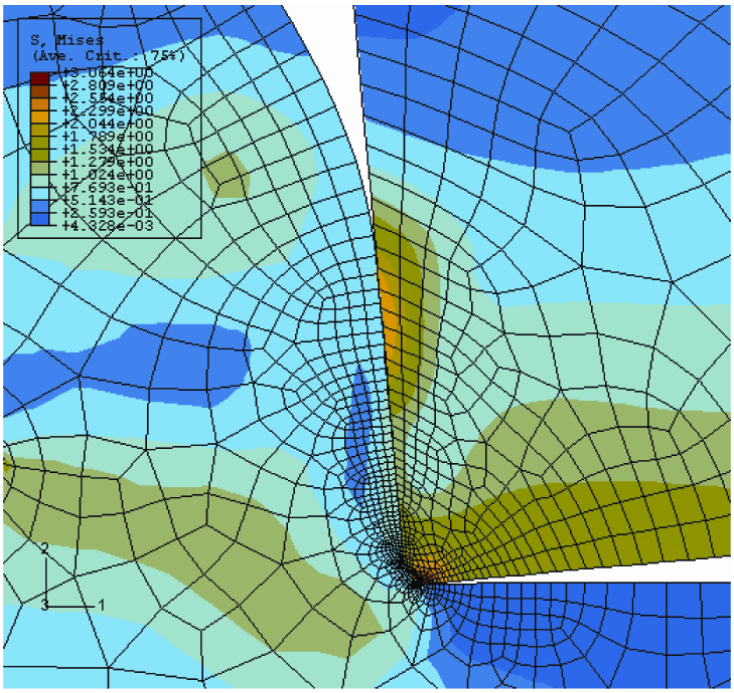

**Figure 10** Machining induced stress distributions of $\sigma_{xx}$ and $\sigma_{yy}$ with respect to depth beneath the machined surface ($t_u$ = 0.1 mm, $V$ = 300 m/min)

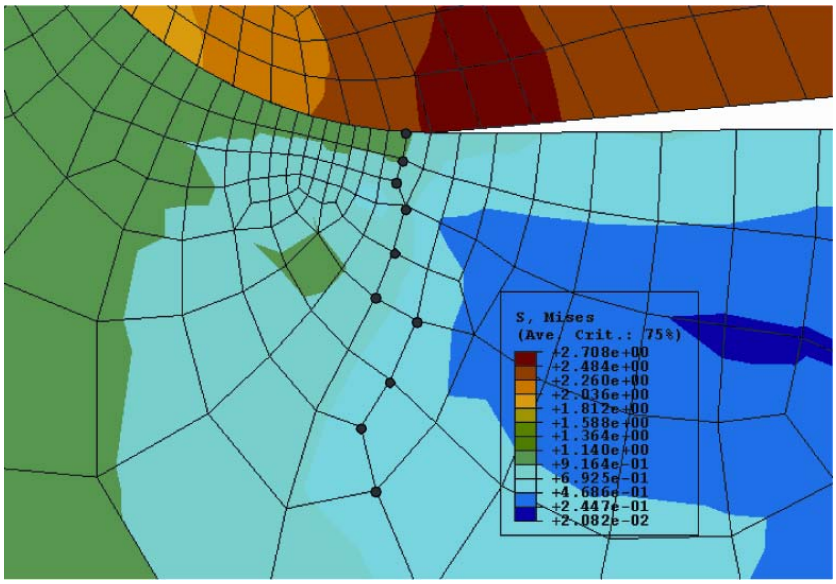


The machining induced state of stress is the highest in machining of AISI 1045 steel and AISI 1045 steel. However, the von Misses stress is significantly lower on the machined layer in machining of Ti6Al4V titanium alloy as shown in Figure 11. On the other hand, process induced stress profiles depict that there exist both compressive and tensile stress regions beneath the surface as shown in Figure 12. In case of machining Ti6Al4V titanium alloy, the stress $\sigma_{xx}$ is compressive indicating preferred surface integrity. However, this stress component is mainly tensile in machining of AISI 1045 steel. All of the work material machined reveals compressive machining induced stress component $\sigma_{yy}$ as shown in Figure 13.

**Figure 11** Machining induced Von Mises stress distributions with respect to depth beneath the machined layer ($t_u$ = 0.1 mm, $V$ = 300 m/min)

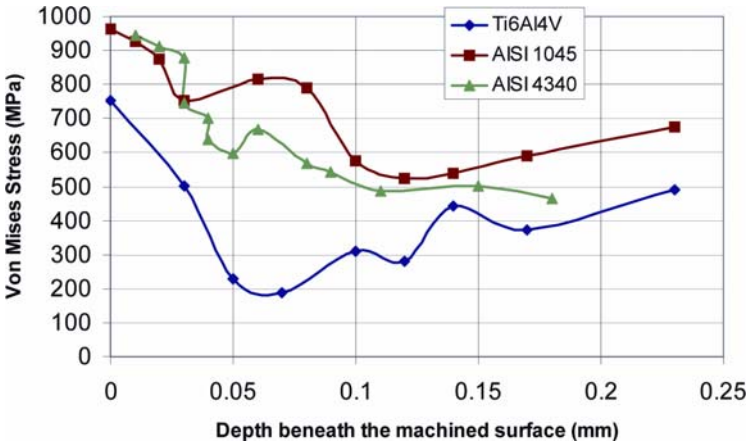

**Figure 12** Machining induced stress distributions of $\sigma_{xx}$ with respect to depth beneath the machined layer ($t_u = 0.1$ mm, $V = 300$ m/min)

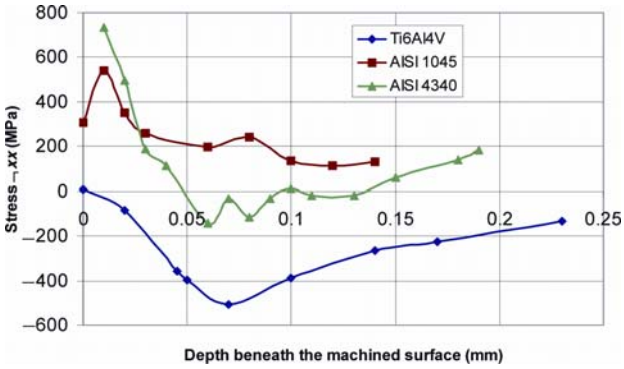


**Figure 13** Machining induced stress distributions of $\sigma_{yy}$ with respect to depth beneath the machined layer ($t_u = 0.1$ mm, $V = 300$ m/min)

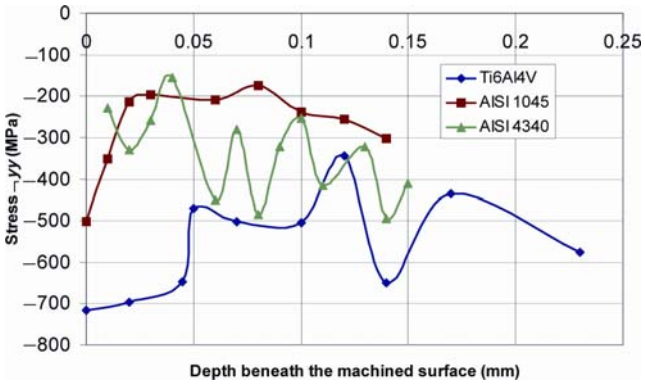


The temperature along the prescribed path is significantly high in machining of Ti6Al4V titanium alloy due to low thermal conductivity as shown in Figure 14 and indicates that there is a possibility of thermo-mechanical processing occurring underneath the round edge tool during machining.

**Figure 14** Temperature distributions of along the prescribed path in the machined layer ($t_u = 0.1$ mm, $V = 300$ m/min)

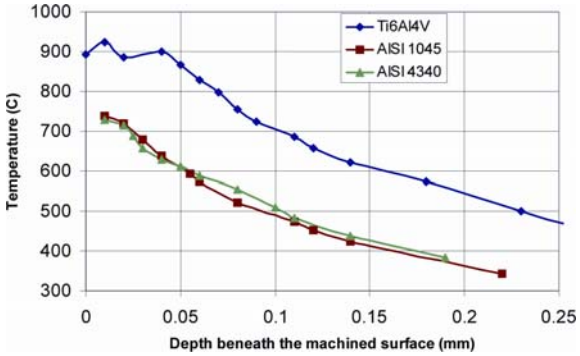

In summary, these stress field predictions can be combined with the temperature field predictions and can be fed into surface property models that are highly essential to further predict surface integrity and thermo-mechanical deformation related property alteration on the microstructure of the machined surfaces. Today, most of the surface property models are empirical and still not sufficient to determine the full surface morphology induced by the finish machining especially at meso-scale where all of the machining is done with the edge geometry of the cutting tool.

## 4 Conclusions

We present a numerical modelling approached based on explicit dynamic Arbitrary Lagrangian Eulerian method with adaptive meshing capability and developed simulation models for meso-scale finish machining of AISI 1045, AISI 4340 steels and Ti6Al4V titanium alloy using finite edge radius carbide cutting tool without employing a remeshing scheme and without using a chip separation criterion. The extended J-C work material model and a detailed friction models are also employed and work material flow around the round edge of the cutting tool is simulated in conjunction with an adaptive meshing scheme. The development of temperature distributions during the cutting process is also captured. Very high and localised temperatures are predicted at tool-chip interface due to a detailed friction model. Predictions of the von Mises stress distributions in the chip, in the tool and on the machined surface are effectively carried out. Process induced stress profiles depict that there exist both compressive and tensile stress regions beneath the surface. These predictions combined with the temperature field predictions are highly essential to further predict surface integrity and thermo-mechanical deformation related property alteration on the microstructure of the machined surfaces. It is believed that the ALE simulation approach presented in this work, without remeshing and using a chip separation criterion, may result in better predictions for finish machining induced stress fields.

## References

Adibi-Sedeh, A.H. and Madhavan, V. (2003) 'Understanding of finite element analysis results under the framework of Oxley's machining model', *Proceedings of the 6th CIRP International Workshop on Modelling of Machining Operations*, Hamilton, Canada.

Astakhov, V.P. (1999) *Metal Cutting Mechanics*, Boca Raton, FL, USA: CRC Press.

Baker, M., Rosler, J. and Siemers, C. (2002) 'A finite element model of high speed metal cutting with adiabatic shearing', *Computers and Structures*, Vol. 80, pp.495–513.

Black, J.T. and Huang, J.M. (1996) 'An evaluation of chip separation criteria for the fem simulation of machining', *ASME Journal of Manufacturing Science and Engineering*, Vol. 118, pp.545–553.

Byrne, G., Dornfeld, D. and Denkena, B. (2003) 'Advancing cutting technology', *Annals of the CIRP, STC C, 52/2/2003*, pp.483–508.

Ceretti, E., Fallböhmer, P., Wu, W.T. and Altan, T. (1996) 'Application of 2-D FEM to chip formation in orthogonal cutting', *Journal of Materials Processing Technology*, Vol. 59, pp.169–181.

Childs, T.H.C., Maekawa, K., Obikawa T. and Yamane, Y. (2000) *Metal Machining Theory and Applications*, London: Butterworth-Heinemann.

Chuzhoy, L., DeVor, R.E. and Kapoor, S.G. (2003) 'Machining simulation of ductile iron and its constituents. Part 2: numerical simulation and experimental validation of machining', *ASME Journal of Manufacturing Science and Engineering*, Vol. 125, pp.192–201.

Davies, M.A., Cao, Q., Cooke, A.L. and Ivester, R. (2003) 'On the measurement and prediction of temperature fields in machining of AISI 1045 steel', *Annals of the CIRP*, Vol. 52, No. 1, pp.77–80.

Deshayes, L., Ivester, R., Mabrrouki, T. and Rigal, J-F. (2004) 'Serrated chip morphology and comparison with finite element simulations', *Proceedings of IMECE'04, 2004 ASME International Mechanical Engineering Congress and Exposition*, 13–20 November, Anaheim, CA, USA.

Dirikolu, M.H., Childs, T.H.C. and Maekawa, K. (2001) 'Finite element simulation of chip flow in metal machining', *International Journal of Mechanical Sciences*, Vol. 43, pp.2699–2713.

Dornfeld, D., Min, S. and Takeuchi, Y. (2006) 'Recent advances in mechanical micromachining', *Annals of the CIRP, STC C, 55/2/2006*.

Guo, Y.B. and Liu, C.R. (2002) '3D FEA modeling of hard turning', *ASME Journal of Manufacturing Science and Engineering*, Vol. 124, pp.189–199.

Guo, Y.B. and Wen, Q. (2005) 'A hybrid modeling approach to investigate chip morphology transition with the stagnation effect by cutting edge geometry', *Transactions of NAMRI/SME*, Vol. 33, pp.469–476.

Haglund, A.J., Kishawy, H.A. and Rogers, R.J. (2005) 'On friction modeling in orthogonal machining: an Arbitrary Lagrangian-Eulerian finite element model', *Transactions of NAMRI/SME*, Vol. 33, pp.589–596.

Ikawa, N., Shimada, S. and Tanaka, H. (1992) 'Minimum thickness of cut in micromachining', *Nanotechnology*, Vol. 3, No. 1, pp.6–9.

Jaspers, S.P.F.C. and Dautzenberg, J.H. (2002) 'Material behavior in conditions similar to metal cutting: flow stress in the primary shear zone', *Journal of Materials Processing Technology*, Vol. 122, pp.322–330.

Johnson, G.R. and Cook, W.H. (1983) 'A constitutive model and data for metals subjected to large strains, high strain rates and high temperatures', *Proceedings of the 7th International Symposium on Ballistics*, The Netherlands: The Hague, pp.541–547.

Joshi, S.S. and Melkote, S.N. (2004) 'An explanation for the size-effect in machining using strain gradient plasticity', *ASME Journal of Manufacturing Science and Engineering*, Vol. 126, No. 4, pp.679–684.

Klocke, F., Raedt, H.W. and Hoppe, S. (2001) '2D-FEM simulation of the orthogonal high speed cutting process', *Machining Science and Technology*, Vol. 5, No. 3, pp.323–340.

Komvopoulos, K. and Erpenbeck, S.A. (1991) 'Finite element modeling of orthogonal metal cutting', *ASME Journal of Engineering for Industry*, Vol. 113, pp.253–267.

Lee, W.B. and Zhou, M (1993) 'A theoretical analysis of the effect of crystallographic orientation on chip formation in micro-machining', *International Journal of Machine Tools and Manufacture*, Vol. 33, pp.439–447.

Leopold, J., Semmler, U. and Hoyer, K. (1999) 'Applicability, robustness and stability of the finite element analysis in metal cutting operations', *Proceedings of the 2nd CIRP International Workshop on Modelling of Machining Operations*, Vols. 81–94, Nantes, France, January.

Li, X. (1997) 'Development of a predictive model for stress distributions at the tool-chip interface in machining', *Journal of Materials Processing Technology*, Vol. 63, pp.169–174.

Lin, Z.C. and Lin, S.Y. (1992) 'A couple finite element model of thermo-elastic-plastic large deformation for orthogonal cutting', *ASME Journal of Engineering for Industry*, Vol. 114, pp.218–226.

Liu, C.R. and Guo, Y.B. (2000) 'Finite element analysis of the effect of sequential cuts and tool-chip friction on residual stresses in a machined layer', *International Journal of Mechanical Sciences*, Vol. 42, pp.1069–1086.

Liu, X., DeVor, R.E. and Kapoor, S.G. (2006) 'An analytical model for the prediction of minimum chip thickness in micromachining', *ASME Journal of Manufacturing Science and Engineering*, Vol. 128, pp.474–481.

Lucca, D.A. and Seo, Y.W. (1993) 'Effect of tool edge geometry on energy dissipation in ultra precison machining', *Annals of the CIRP*, Vol. 42, No. 1, pp.83–86.

Madhavan, V., Chandrasekar, S. and Farris, T.N. (2000) 'Machining as a wedge indentation', *Journal of Applied Mechanics*, Vol. 67, pp.128–139.

Marusich, T.D. and Ortiz, M. (1995) 'Modeling and simulation of high-speed machining', *International Journal for Numerical Methods in Engineering*, Vol. 38, pp.3675–3694.

Melkote, S.N. and Endres, W.J. (1998) 'The importance of including the size effect when modeling slot milling', *ASME Journal of Manufacturing Science and Engineering*, Vol. 120, pp.68–75.

Meyer Jr., H.W. and Kleponis, D.S. (2001) 'Modeling the high strain rate behavior of titanium undergoing ballistic impact and penetration', *International Journal of Impact Engineering*, Vol. 26, pp.509–521.

Movahhedy, M.R., Altintas, Y. and Gadala, M.S. (2002) 'Numerical analysis of metal cutting with chamfered and blunt tools', *ASME Journal of Manufacturing Science and Engineering*, Vol. 124, pp.178–188.

Movahhedy, M.R., Gadala, M.S. and Altintas, Y. (2000) 'FE modeling of chip formation in orthogonal metal cutting process: an ALE approach', *Machining Science and Technology*, Vol. 4, pp.15–47.

Ng, E.G., Tahany, I.E.W., Dumitrescu, M. and Elbastawi, M.A. (2002) 'Physics-based simulation of high speed machining', *Machining Science and Technology*, Vol. 6, No. 3, pp.301–329.

Olovsson, L., Nilsson, L. and Simonsson, K. (1999) 'An ALE formulation for the solution of two-dimensional metal cutting problems', *Computers and Structures*, Vol. 72, pp.497–507.

Outeiro, J.C. and Astakhov, V.P. (2005) 'The role of the relative tool sharpness in modelling of the cutting process', *Proceedings of the 8th CIRP International Workshop on Modeling of Machining Operations*, Chemnitz, Germany, pp.517–523.

Özel, T. (2003) 'Modeling of hard part machining: effect of insert edge preparation for CBN cutting tools', *Journal of Materials Processing Technology*, Vol. 141, pp.284–293.

Özel, T. (2006) 'Influence of friction models on finite element simulations of machining', *International Journal of Machine Tools and Manufacture*, Vol. 46, No. 5, pp.518–530.

Özel, T. and Altan, T. (2000) 'Determination of workpiece flow stress and friction at the chip-tool contact for high-speed cutting', *International Journal of Machine Tools and Manufacture*, Vol. 40, No. 1, pp.133–152.

Özel, T. and Zeren, E. (2005a) 'Finite element method simulation of machining of AISI 1045 steel with a round edge cutting tool', *Proceedings of the 8th CIRP International Workshop on Modeling of Machining Operations*, Chemnitz, Germany, pp.533–542.

Özel, T. and Zeren, E. (2005b) 'Finite element modeling of stresses induced by high speed machining with round edge cutting tools', *Proceedings of IMECE'05, 2005 ASME International Mechanical Engineering Congress and Exposition*, Paper No. 81046, Orlando, FL, 5–11 November.

Özel, T. and Zeren, E. (2006) 'A methodology to determine work material flow stress and tool-chip interfacial friction properties by using analysis of machining', *ASME Journal of Manufacturing Science and Engineering*, Vol. 128, No. 1, pp.119–129.

Rakotomalala, R., Joyot, P. and Touratier, M. (1993) 'Arbitrary Lagrangian-Eulerian thermomechanical finite element model of material cutting', *Communications in Numerical Methods in Engineering*, Vol. 9, pp.975–987.

Schmidt, J. and Tritschler, H. (2004) 'Micro cutting of steel', *Microsystem Technologies*, Vol. 10, pp.167–174.

Sekhon, G.S. and Chenot, J.L. (1992) 'Some simulation experiments in orthogonal cutting', *Numerical Methods in Industrial Forming Processes*, pp.901–906.

Shih, A.J. (1995) 'Finite element simulation of orthogonal metal cutting', *ASME Journal of Engineering for Industry*, Vol. 117, pp.84–93.

Strenkowski, J.S. and Carroll, J.T. (1985) 'A finite element model of orthogonal metal cutting', *ASME Journal of Engineering for Industry*, Vol. 107, pp.346–354.

Strenkowski, J.S. and Carroll, J.T. (1986) 'Finite element models of orthogonal cutting with application to single point diamond turning', *International Journal of Mechanical Science*, Vol. 30, pp.899–920.

Tönshoff, H.K., Arendt, C. and Ben Amor, R. (2000) 'Cutting of hardened steel', *Annals of the CIRP, STC C, 49/2/2000*, pp.547–551.

Usui, E. and Shirakashi, T. (1982) 'Mechanics of machining -from descriptive to predictive theory. In on the art of cutting metals-75 years later', *ASME Publication PED*, Vol. 7, pp.13–35.

Weule, H., Huntrup, V. and Tritschle, H. (2001) 'Micro-cutting of steel to meet new requirements in miniaturization', *Annals of the CIRP*, Vol. 50, No. 1, pp.61–64.

Yang, X. and Liu, C.R. (2002) 'A new stress-based model of friction behavior in machining and its significant impact on residual stresses computed by finite element method', *International Journal of Mechanical Sciences*, Vol. 44, No. 4, pp.703–723.

Yen, Y-C., Jain, A. and Altan, T. (2004) 'A finite element analysis of orthogonal machining using different toll edge geometries', *Journal of Material Processing Technology*, Vol. 146, No. 1, pp.72–81.

Zhang, B. and Bagchi, A. (1994) 'Finite element simulation of chip formation and comparison with machining experiment', *ASME Journal of Engineering for Industry*, Vol. 116, pp.289–297.

Zorev, N.N. (1966) *Metal Cutting Mechanics*, Oxford, UK: Pergamon Press.